Biochimica et Biophysica Acta 1852 (2015) 2574–2584

Contents lists available at ScienceDirect

Biochimica et Biophysica Acta

journal homepage: www.elsevier.com/locate/bbadis

GSK3β and Gli3 play a role in activation of Hedgehog-Gli pathway in human colon cancer — Targeting GSK3β downregulates the signaling pathway and reduces cell proliferation

Diana Trnski [a], Maja Sabol [a], Ante Gojević [b], Marina Martinić [a], Petar Ozretić [a], Vesna Musani [a], Snježana Ramić [c], Sonja Levanat [a,*]

[a] Department of Molecular Medicine, Rudjer Boskovic Institute, Bijenička 54, Zagreb, Croatia
[b] Department of Surgery, University Hospital Center Zagreb, Kišpatićeva 12, Zagreb, Croatia
[c] Department of Pathology, University Hospital for Tumors, Sestre milosrdnice University Hospital Center, Ilica 197, Zagreb, Croatia

ARTICLE INFO

Article history:
Received 15 June 2015
Received in revised form 4 September 2015
Accepted 12 September 2015
Available online 15 September 2015

Keywords:
Hedgehog signaling
Gli3
GSK3β
Autophagy
Apoptosis
Colon cancer

ABSTRACT

The role of Hedgehog-Gli (Hh-Gli) signaling in colon cancer tumorigenesis has not yet been completely elucidated. Here we provide strong evidence of Hh-Gli signaling involvement in survival of colon cancer cells, with the main trigger of activation being deregulated GSK3β.

Our clinical data reveals high expression levels of GSK3β and Gli3 in human colon cancer tissue samples, with positive correlation between GSK3β expression and DUKES' stage. Further experiments on colon cancer cell lines have shown that a deregulated GSK3β upregulates Hh-Gli signaling and positively affects colon cancer cell survival. We show that inhibition of GSK3β with lithium chloride enhances Gli3 processing into its repressor form, consequently downregulating Hh-Gli signaling, reducing cell proliferation and inducing cell death. Analysis of the molecular mechanisms revealed that lithium chloride enhances Gli3–SuFu–GSK3β complex formation leading to more efficient Gli3 cleavage and Hh-Gli signaling downregulation. This work proposes that activation of the Hh-Gli signaling pathway in colon cancer cells occurs non-canonically via deregulated GSK3β. Gli3 seems to be the main pathway effector, highlighting the activator potential of this transcription factor, which is highly dependent on GSK3β function and fine tuning of the Gli3–SuFu–GSK3β platform.

1. Introduction

The Hh-Gli signaling pathway acts as a mitogen, morphogen and differentiation factor in embryonic development and is involved in major processes during gastrointestinal (GI) development [1,2]. The canonical pathway is activated by binding of the ligand Hedgehog (Hh) to the transmembrane receptor Patched (Ptch), which triggers their internalization. As a consequence, Smoothened (Smo) is translocated to the cell membrane where it triggers a signaling cascade, ultimately leading to the release of Gli transcription factors from SuFu and its translocation to the nucleus. Gli1 is an activator of the pathway, while Gli2 and Gli3 act as activators or repressors, depending on the cellular context [3]. In the absence of Hh signal, Gli1 is degraded, while Gli2 and Gli3 are processed into transcriptional repressors [4–6]. Hh-Gli signaling target genes are involved in proliferation and differentiation, cell survival, self-renewal, angiogenesis, and autoregulation of the pathway [7–9].

SuFu, a negative regulator of the pathway, binds Gli proteins and prevents their translocation to the nucleus [10,11]. It interacts with a conserved motif on the Gli protein, and enables Gli phosphorylation by PKA, GSK3β and CK1 [12]. GSK3β is a multifunctional serine/threonine kinase involved in metabolic and developmental pathways, and many cellular functions such as stem cell differentiation, self-renewal and apoptosis [13]. The role of GSK3β in the Hh-Gli signaling pathway is twofold: phosphorylation of Gli proteins, tagging them for degradation and processing into repressor forms in the inactive state, or binding SuFu in ligand-stimulated cells and enabling the release of Gli from the complex [14]. GSK3β is mainly regulated through posttranslational phosphorylation events, an activating phosphorylation at Tyr216 and an inhibitory phosphorylation at Ser9 [15]. Under resting conditions GSK3β is constitutively active and its activity is regulated through a balance between the levels of activating and inhibiting phosphorylations [16–18].

In some cancer types, inactivation of GSK3β leads to tumorigenesis. In contrast to its tumor-suppressing activity in these cell types, GSK3β protein overexpression and pro-survival role have been found in several

* Corresponding author at: Division of Molecular Medicine, Rudjer Boskovic Institute, 10000 Zagreb, Croatia.
E-mail addresses: diana.trnski@irb.hr (D. Trnski), maja.sabol@irb.hr (M. Sabol), ante.gojevic@xnet.hr (A. Gojević), marina.martinic.87@gmail.com (M. Martinić), pozretic@irb.hr (P. Ozretić), vmusani@irb.hr (V. Musani), snjezana.ramic@zg.t-com.hr (S. Ramić), levanat@irb.hr (S. Levanat).

http://dx.doi.org/10.1016/j.bbadis.2015.09.005
0925-4439/

human cancer cells, including colon cancer [19]. Higher levels of GSK3β and its active isoform were reported in colon cancer tumors compared with normal tissues, while the inactive form, phosphorylated at Ser9, was mostly detected in non-neoplastic tissues [20]. Even though the results suggest that GSK3β may participate in colon cancer development, the mechanism has not been discovered. Here we describe a potential mechanism underlying the oncogenic role of GSK3β through deregulation of the Hh-Gli signaling pathway. By keeping it in an active state, it contributes to colon cancer cell proliferation.

2. Materials and methods

2.1. Colon cancer tissue samples

Twenty tissue samples from colon carcinoma patients were collected from the Clinical Hospital Center Zagreb. Relevant clinical data is listed in Table 1. All experiments were performed in accordance with the Declaration of Helsinki, and the Ethical Committee of Clinical Hospital Center Zagreb no. 01/001/VG (dated November 29, 2010) approved the study. Tissue samples were routinely paraffinized and sliced into 5 μm sections for immunohistochemical staining.

2.2. Immunohistochemistry

Paraffin slides were deparaffinized, rehydrated and boiled in Target Retrieval solution (Dako, S2367) using PTlink (Dako). Primary antibodies anti-Shh (sc-9024), anti-Ptch1 (sc-6147), anti-Smo (sc-13,943), anti-SuFu (sc-10,933), anti-GSK3β (sc-8257), anti-Gli1 (sc-20,687), anti-Gli2 (sc-20,291) and anti-Gli3 (sc-20,688) from Santa Cruz Biotechnology (SCBT) were used at a 1:50 dilution, +4 °C, overnight. Slides were stained on the Dako autostainer using the Dako LSAB+/HRP kit (Dako, K0679). For negative control, slides were treated identically, omitting the primary antibody step. Slides were visualized using the Olympus CX41 RF microscope and images were taken with the Olympus Digital camera C-5060.

Relative DAB staining intensity was quantified using a cyan-magenta-yellow-black (CMYK) color model adapted from Pham et al.[21], which was successfully applied in several studies [22,23].

2.3. Cell culture

SW480, HCT116 and Caco-2 colon cancer cell lines, derived from primary colorectal adenocarcinomas and the SW620 cell line, derived from a metastasis of the primary tumor from which SW480 was derived, were used for cell culture experiments. Cells were cultured in Dulbecco's Minimal Essential Medium (DMEM) supplemented with 10% fetal bovine serum (PAA), 200 mM of sodium pyruvate and 2 mM of L-glutamine, and were maintained in a humidified 5% CO_2 environment. For gene and protein expression experiments, 24 h after seeding, cells were treated with 10 μM of cyclopamine (Toronto Research Chemicals) for 48 h, 20–40 mM of lithium chloride (LiCl) (Kemika) for 24 and 48 h, 0.5 μM of SAG (SCBT) for 24 h, with DMSO treatment as vehicle control. For the analysis of the effect of SAG on GSK3β Ser9 phosphorylation, cells were treated with DMSO as vehicle control, 30 mM of LiCl, 0.5 μM of SAG, 1 μM of SAG and combined treatments of 30 mM of LiCl with 0.5 μM of SAG or 1 μM of SAG for 24 h. For analysis of caspase-3 and PARP cleavage cells were treated with 20–40 mM of LiCl for 72 h. For analysis of LC3 processing cells were treated with either 30 mM of LiCl, 30 mM of LiCl after 1 h of pre-incubation with 10 mM of ammonium-chloride (NH_4Cl) (Kemika) or 10 mM of NH_4Cl alone for 4 h.

2.4. GSK3β silencing

Cells in 6-well plates were transfected with 50 nM of GSK3β siRNA (sc-35,527, SCBT) or Silencer Negative Control #1 siRNA (Life Technologies) using siPORT NeoFX (Life Technologies) transfection reagent. The medium was changed after 24 h, and cells were collected after an additional 24 h.

2.5. Cell proliferation assay

Cell proliferation and viability was determined using MTT assay. Briefly, cells in 96-well plates were treated in quadruplicates for 72 h with 2.5–15 μM of Smo inhibitor cyclopamine or 10–50 mM of GSK3β inhibitor LiCl. The effect of SAG (0.25, 0.5, 1 and 2 μM) was analyzed after 24, 48 and 72 h. To analyze if SAG can rescue the effect of LiCl, cells were treated simultaneously with LiCl (30 mM or 40 mM) and increasing concentrations of SAG (0.25, 0.5, 1 and 2 μM) for 24, 48 and

Table 1
Relevant clinical data for the colon carcinoma patients.

Sample no.	Diagnosis	Grade	DUKES'	Age	Positive lymph nodes	CEA[a]	Size
Sample no.	Diagnosis	Grade	DUKES'	Age	Positive lymph nodes	CEA[a]	Size
1	Ca sygmae	1	B	73	0	3	42 mm
2	Ca coli ascedens	1	B	78	0	3,2	50 mm
3	Ca sygmae	1	C	73	1	4,49	40 mm
4	Ca recti	1	C	59	1	1,82	65 mm
5	Ca sygmae	1	A	65	0	2,8	46 mm
6	Ca coli transversi	1	C	56	1	10,52	45 mm
7	Ca coli transversi	1	D	79	1	10,22	60 mm
8	Ca recti	1	C	61	1	3,2	45 mm
9	Ca coli descedens	1	C	60	1	2,9	36 mm
10	Ca sygmae	3	C	50	1	0,98	40 mm
11	Ca coli ascedens	1	C	70	1	3	40 mm
12	Ca coli ascedens	1	A	53	0	1,6	62 mm
13	Ca sygmae	1	C	70	1	3,6	40 mm
14	Ca coli ascedens	1	B	49	0	2,2	42 mm
15	Ca sygmae	1	D	73	1	75,95	42 mm
16	Ca coeci	1	A	74	0	2,8	42 mm
17	Ca sygmae	1	C	70	1	2,14	40 mm
18	Ca recti	1	B	76	0	3,74	40 mm
19	Ca sygmae	1	A	73	0	3,24	45 mm
20	Ca recti	1	C	58	1	7,66	60 mm

[a] CEA — carcinoembryonic antigen.

72 h. The medium was then removed, and cells were incubated with MTT solution (1 mg/ml) for 4 h. DMSO was used to dissolve the formazan product. Absorbance was measured at 570 nm.

2.6. Quantitative real-time PCR (qRT-PCR)

RNA was extracted from cells using TRIzol reagent (Invitrogen) according to manufacturer's instructions. 1 μg of RNA was reverse transcribed into cDNA using TaqMan Reverse Transcription Reagents (Applied Biosystems). Gene expression experiments were performed in the CFX96 real-time PCR machine (Bio-Rad) using Sso Fast EvaGreen Supermix (Bio-Rad) and the following primers: *RPLP0* F 5' GGCACCATTG AAATCCTGAGTGATGTG 3', *RPLP0* R 5' TTGCGGACACCCTCCAGGAAGC 3', *PTCH1* F 5' TCCTCGTGTGCGCTGTCTTCCTTC 3', *PTCH1* R 5' CGTCAGAAAG GCCAAAGCAACGTGA 3', *SMO* F 5' CTGGTACGAGGACGTGGAGG 3', *SMO* R 5' AGGGTGAAGAGCGTGCAGAG 3', *GLI1* F 5' GCCGTGTAAAGCTCCAGT GAACACA 3', *GLI1* R 5' TCCCACTTTGAGAGGCCCATAGCAAG 3', *SHH* F 5' GAAAGCAGAGAACTCGGTGG 3', *SHH* R 5' GGTAAGTGAGGAAGTCGCTG 3' [24], *SUFU* F 5' AACAGCAAACCTGTCCTTCC 3', *SUFU* R 5' TCAGATGT ACGCTCTCAAGC 3' [25], *GLI2* F 5'-GCCATCAAGACCGAGAGCTC-3', *GLI2* R5'-CGGCCCATGAGCAGGAATCC-3' [26], *GLI3* F 5'-CACTACCTCAAAGC GGGAAG-3', *GLI3* R 5'-TGTTGGACTGTGTGCCATTT-3' [27], *GSK3β* F 5'-GGAGAACTGGTCGCCATCAAG-3', *GSK3β* R 5'-ACATTGGGTTCTCCTCGG ACC-3'[28].

2.7. Western blot

Proteins were extracted from cells using RIPA buffer supplemented with protease inhibitors (Roche) with addition of phosphatase inhibitors (Roche) for phosphorylated protein extraction. Protein concentration was determined using Bio-Rad Protein Assay (Bio-Rad). For analysis, 50 μg of protein was used. Membranes were blocked in 5% milk. Primary antibodies against Gli3 (sc-20,688, SCBT; AF-3690, R&D Systems; 19,949–1-AP, ProteinTech), GSK3β (#9832, Cell Signaling Technology (CST)), phospho-Ser9 GSK3β (#5558, CST), Sufu (#2520, CST) and Ptch1 (sc-6147, SCBT; 17,520–1-AP, ProteinTech) were used. For LC3 detection the MAP LC3α/β antibody was used (sc-292,354, SCBT). For apoptosis the anti-PARP (556,362, BD Pharmingen) and the anti-caspase-3 (sc-7272, SCBT) antibodies were used. Actin (sc-1616, SCBT) was used as loading control. After washing, membranes were incubated with the appropriate secondary HRP-conjugated antibody. Proteins were visualized using Super Signal West Pico and Super Signal West Femto reagents (Pierce).

2.8. Co-immunoprecipitation

Co-immunoprecipitation was performed using Protein G coated Dynabeads (Life Technologies) according to the manufacturer's instructions (Invitrogen, Rev. 005). For Gli3 co-immunoprecipitation 4 μg of Gli3 antibody (AF-3690, R&D) was used per sample. For SuFu and GSK3β co-immunoprecipitations, SuFu (#2520, CST) and GSK3β (#9832, CST) antibodies were used at a 1:25 dilution. Samples were incubated with the Dynabead–antibody complex over night at +4 °C. Samples were eluted with 1× loading buffer and heated 5 min at 95 °C before analysis on Western blot.

2.9. Acridine orange staining and flow cytometric analysis

For analysis of AVO, cells grown in triplicate in 12-well plates were treated with 20, 30 and 40 mM LiCl for 72 h. Then, 2 μg/ml of acridine orange in serum free medium was added for 30 min, after which the cells were washed in PBS and trypsinized. Cells were then pelleted, resuspended in PBS containing 2 μg/ml of acridine orange and analyzed by flow cytometry (BD FACSCalibur).

2.10. Immunofluorescence

Immunofluorescent staining and confocal microscopy was performed as previously described [29]. Primary antibodies for Gli3 and GSK3β, were the same as for co-IP experiments. Confocal images were examined using the Mander's coefficient plug-in of the ImageJ software (v 1.45e) for co-localization of green and red signals.

2.11. Colony formation assay

10^3 cells were seeded per well in a 6-well plate. The following day the cells were treated with 20 and 30 mM of LiCl. Colonies were grown for 2 weeks and medium with treatment was changed every three days. Colonies were fixed with formaldehyde and stained using 1% cristal violet.

2.12. Statistical analysis

For gene expression, all experiments were performed at least in duplicates and mean values and standard error was calculated for each data point. For immunohistochemical staining, $\chi 2$ test was used to determine the association between variables. One way ANOVA was used for autophagy analysis and the analysis of difference in co-localization between untreated samples and each treatment. All two-tailed P-values less than 0.05 were considered statistically significant. The analysis was performed using MedCalc for Windows version 11.4.2.0 (MedCalc Software, Mariakerke, Belgium).

3. Results

3.1. Tissue expression of GSK3β and Gli3 correlate with clinical parameters

Twenty colon cancer tissue samples were stained for Hh-Gli pathway proteins Ptch, Smo, Gli1, Gli2, Gli3, Shh, SuFu and GSK3β. Of the 20 samples, 19 samples were of grade I and one sample was a grade III tumor. According to DUKES' staging the sample set was consisted of tumors ranging from stage A to stage D (Table 1). GSK3β and Gli3 showed high staining intensities (2 and 3) in 95% of samples (Fig. 1, Table 2). 90% of samples showed no Smo staining and 65% no Ptch staining (Table 2). Staining intensities were compared with several clinical parameters: DUKES' stage, positivity of surrounding lymph nodes, or carcinoembryonic antigen (CEA) expression. Fifteen lymph nodes were examined for each of the patients, and a positive score was given if at least one of them was positive for transformed cells. GSK3β staining was correlated with DUKES' stage ($P = 0.034$) with higher DUKES' stages more strongly stained for GSK3β. For Gli3, a similar trend was visible, but not statistically significant ($P = 0.058$). The sample number needs to be increased in order to confirm the correlation of Gli3 and DUKES' stage, but the obtained results suggest a pro-tumorigenic role for GSK3β in these samples.

3.2. Hh-Gli pathway is active in human colon cancer cells

Four colon cancer cell lines (SW480, SW620, HCT116 and Caco-2) were tested for the presence of *GSK3β* and other Hh-Gli signaling components. Since HCT116 and Caco-2 did not express *GLI3* (Fig. 2A), which according to the results on clinical samples possibly plays a role in colon cancer, we continued our research with SW480 and SW620 cells. We found *SHH*, *PTCH1*, *SMO*, *GSK3β*, *SUFU* and *GLI3* expressions in both cell lines, while *GLI1* and *GLI2* expressions were weaker (Fig. 2A). To confirm the activity of the pathway in these cell lines we tested their responsiveness to the Hh-Gli pathway agonist SAG, as well as a Hh-Gli inhibitor, cyclopamine. The pathway was stimulated in both cell lines after treatment with SAG. SAG induced *PTCH1* and *GLI1* expression but with different modalities in the two cell lines. *PTCH1* induction was more pronounced in SW480 cells, whereas *GLI1* induction was

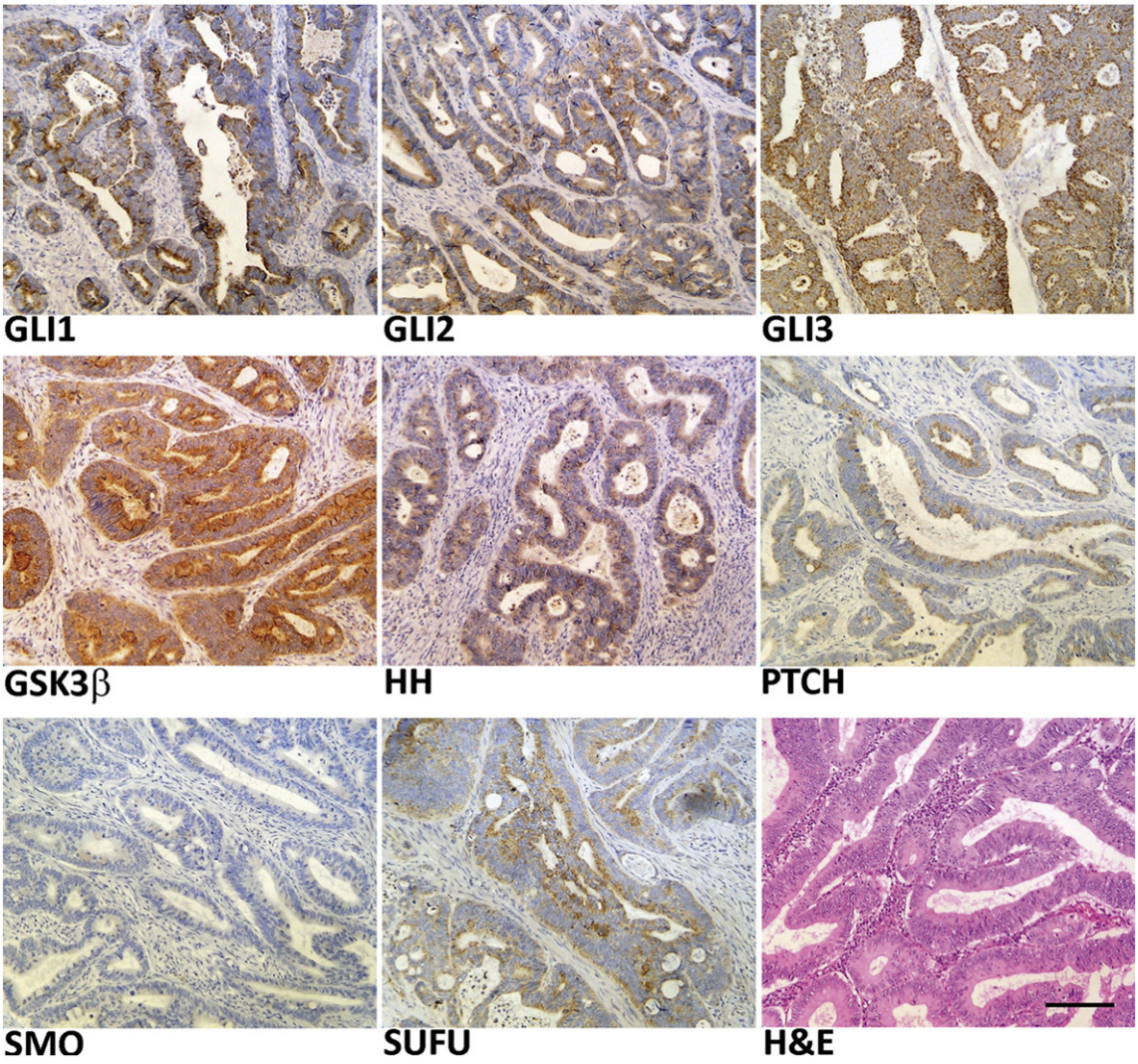

Fig. 1. Immunohistochemical staining of Gli1, Gli2, Gli3, GSK3β, Hh, Ptch, Smo and SuFu in colon cancer tissue samples. Gli3 and GSK3β show the highest staining intensity. Scale bar represents 100 μm.

more pronounced in SW620 cells. In addition, we also observed upregulation of *GLI2* and *GLI3* genes (Fig. 2B). SAG also affected cell proliferation in a dose dependent manner, the proliferation rates of both cell lines increased with increasing SAG concentrations. This effect was more pronounced at the earlier time points, when SAG was shown to have an effect on Hh-Gli signaling activity (Fig. 2 C, D). Cyclopamine, a pathway inhibitor, on the other hand, did not have an inhibitory effect on Hh-Gli pathway activity. On the contrary, it slightly increased PTCH1 and GLI1 expression levels in SW480 cells, and had no effect on target gene expression levels in SW620 cells (Fig. 2E). Cyclopamine also had no effect on cell proliferation in either cell line (Fig. 2F). These results suggest that the pathway can be additionally activated, but inhibition at the level of Smo is not functional.

3.3. Inhibition of GSK3β with LiCl downregulates Hh-Gli signaling and inhibits cell proliferation, whereas GSK3β knock-down upregulates Hh-Gli signaling

We tested the impact of GSK3β inhibition with LiCl on Hh-Gli signaling in SW480 and SW620 cells, as high GSK3β expression in clinical samples and unresponsiveness of the cell lines to the Smo inhibitor cyclopamine were indicative of GSK3β deregulation. GSK3β proved essential for colon cancer cell proliferation and survival, since after treatment with LiCl proliferation of both cell lines decreased in a dose-dependent manner (Fig. 3A). The ability of both cell lines to form colonies was decreased as well, and although 20 mM of LiCl affected colony formation only slightly, 30 mM of LiCl inhibited clonogenic potential

Table 2
Relative staining intensities of tested proteins in colon carcinoma clinical samples. Intensities were determined using the CMYK color model as described by Pham et al.[21].

Staining intensity	PTCH		SMO		GLI1		GLI2		GLI3		HH		SUFU		GSK3β	
	No.	%	No.	%	No.	%	No.	%	No.	%	No.	%	No.	%	no.	%
0	13	65%	18	90%	6	30%	9	45%	1	5%	5	25%	5	25%	1	5%
1	4	20%	2	10%	4	20%	4	20%	0	0%	5	25%	6	30%	0	0%
2	0	0%	0	0%	3	15%	3	15%	5	25%	3	15%	4	20%	3	15%
3	3	15%	0	0%	7	35%	4	20%	14	70%	7	35%	5	25%	16	80%
Total	20	100%	20	100%	20	100%	20	100%	20	100%	20	100%	20	100%	20	100%

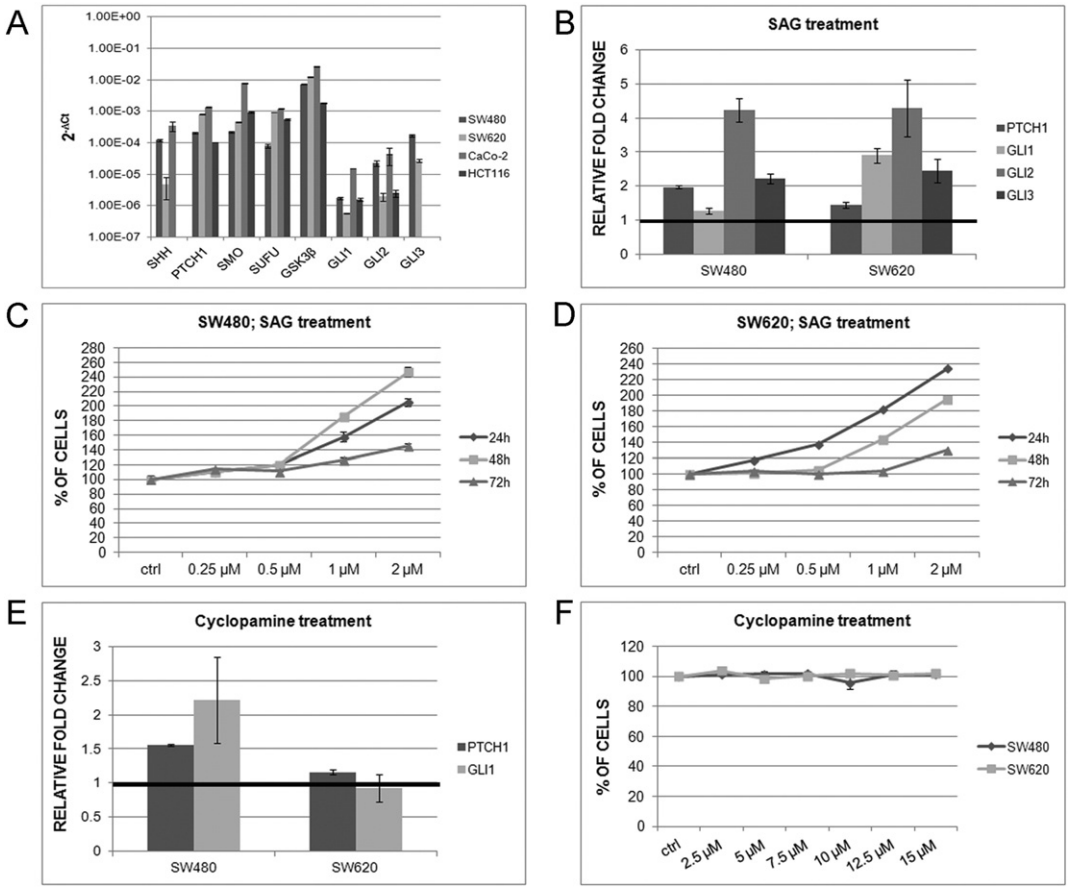

Fig. 2. Hh-Gli signaling is active in human colon cancer cell lines. (A) Basal levels of Hh-Gli components expression normalized relative to expression of the housekeeping gene *RPLP0* and shown as $2^{-\Delta Ct}$ values on logarithmic scale. (B) Effects of 0.5 μM SAG (24 h) on Hh-Gli target gene (*PTCH1*, *GLI1*), *GLI2* and *GLI3* expression relative to expression in control cells with value of 1 (emboldened line). (C, D) SAG increases cell proliferation rates of SW480 and SW620 cell lines. (E) Effects of 10 μM cyclopamine (48 h) on Hh-Gli target gene expression relative to non-treated conditions with value 1 (emboldened line). (F) Effect of increasing doses of cyclopamine on cell proliferation, measured after 72 h.

almost completely (Fig. 3B). GSK3β inhibition with LiCl also led to Hh-Gli signaling downregulation (Fig. 3C). The Hh-Gli target gene *GLI1* was efficiently decreased in both cell lines, whereas *PTCH1* gene expression was downregulated in SW480 but remained unaffected in SW620 cells. Nevertheless, Western blot analysis confirmed decreased Ptch1 protein levels after treatment in both cell lines (Fig. 3D). At the level of Gli transcription factors, we observed significant changes in the equilibrium of Gli3 full length (Gli3FL) and repressor (Gli3R) forms after GSK3β inhibition. In untreated cells, both the Gli3FL and Gli3R forms were present in equal amounts, but after LiCl treatment increased processing of Gli3 protein into its repressor form occurred in both cell lines (Fig. 3E). A decrease in Gli3FL levels, and increasing Gli3R levels, indicate Gli3R as the main inhibitory switch after GSK3β inhibition.

In contrast to inhibiting GSK3β with LiCl, knock-down of its expression in SW480 cells had an opposite effect on Hh-Gli signaling. Gli3FL and Ptch1 protein expression levels were upregulated upon GSK3β knock-down, indicating pathway activation (Fig. 3F).

Interestingly, we have shown that the effects of LiCl (30 mM and 40 mM) on the proliferation rates of both cell lines can be rescued by simultaneously stimulating the Hh-Gli signaling pathway. Again, the effect was more pronounced at earlier time points, when the effect of SAG on Hh-Gli signaling is strongest (Fig. 3G, H).

3.4. LiCl enhances Gli3 cleavage by restoring GSK3β function

The Ser9 phosphorylation of GSK3β is lost in colon cancer cell lines, whereas the activating Tyr216 phosphorylation remains [20]. LiCl is known for promoting the inhibitory Ser9 phosphorylation of GSK3β [30], so we checked the Ser9 phosphorylation status of GSK3β in SW480 and SW620 cells before and after treatment with LiCl compared to total GSK3β levels. Total GSK3β levels remained constant regardless of treatment status but the phosphorylated Ser9 fraction of GSK3β increased after treatment with LiCl (Fig. 4A). We have also shown that stimulating the Hh-Gli signaling pathway with SAG mildly decreases the Ser9 phosphorylated fraction of GSK3β in both cell lines (Fig. 4B), which is in accordance with the observed upregulation of Hh-Gli activity (Fig. 2B). Interestingly, SAG is also able to rescue the effect of LiCl on GSK3β Ser9 phosphorylation in both cell lines, shown by a decreased Ser9 phosphorylated fraction of GSK3β when SAG is added to LiCl, compared with LiCl alone (Fig. 4B). This result confirms that the increase in

Fig. 3. LiCl inhibits cell proliferation and downregulates Hh-Gli signaling. (A) LiCl inhibits SW480 and SW620 cell proliferation in a dose-dependent manner. (B) LiCl affects the colony formation ability of SW480 and SW620 cells; 30 mM of LiCl inhibits this ability almost completely. (C) 20 mM of LiCl downregulates Hh-Gli pathway activity as indicated by decreased levels of target gene expression. Data are represented as fold change ($2^{-\Delta\Delta Ct}$) relative to control cells with the value of 1, plotted on logarithmic scale. (D) Western blot showing decreasing levels of Ptch1 protein after 20 mM of LiCl treatment. (E) Western blot showing that 20 mM of LiCl enhances Gli3 protein processing into repressor form in both cell lines. (F) GSK3β knock-down increases Ptch1 and Gli3FL levels. (G, H) Simultaneous stimulation of Hh-Gli signaling with SAG can rescue the inhibiting effect of LiCl (30 and 40 mM) on cell proliferation rates of both cell lines. The effects are most pronounced at earlier time points when SAG has the strongest effect on Hh-Gli signaling.

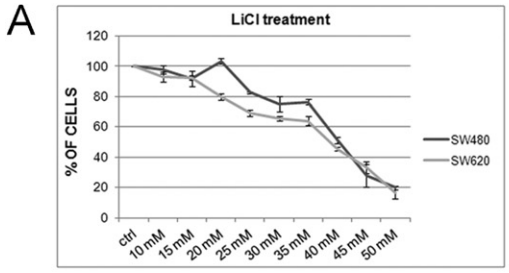
A
LiCl treatment
% OF CELLS
120
100
80
60
40
20
0
ctrl
10 mM
15 mM
20 mM
25 mM
30 mM
35 mM
40 mM
45 mM
50 mM
SW480
SW620

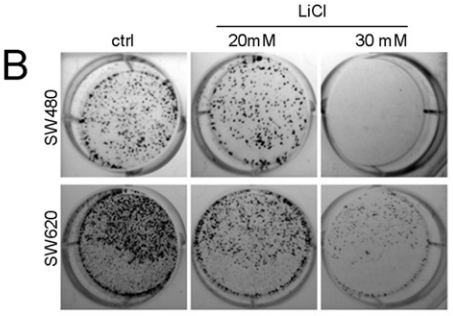
B
LiCl
ctrl
20mM
30 mM
SW480
SW620

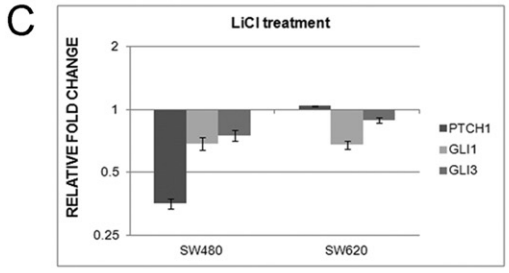
C
LiCl treatment
RELATIVE FOLD CHANGE
2
1
0.5
0.25
SW480
SW620
PTCH1
GLI1
GLI3

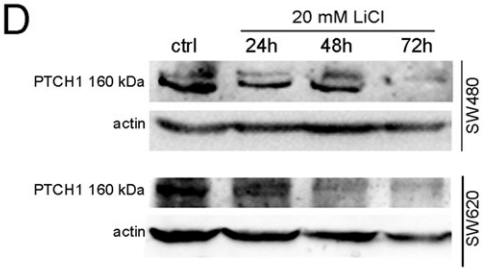
D
20 mM LiCl
ctrl
24h
48h
72h
PTCH1 160 kDa
actin
SW480
PTCH1 160 kDa
actin
SW620

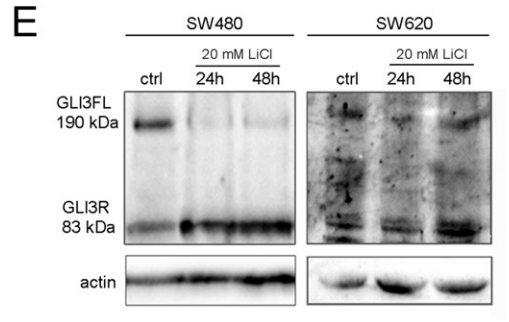
E
SW480
SW620
20 mM LiCl
20 mM LiCl
ctrl
24h
48h
ctrl
24h
48h
GLI3FL
190 kDa
GLI3R
83 kDa
actin

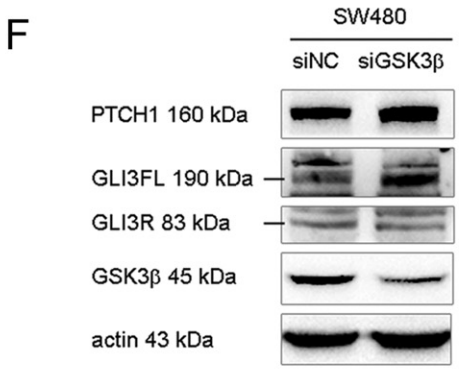
F
SW480
siNC
siGSK3β
PTCH1 160 kDa
GLI3FL 190 kDa
GLI3R 83 kDa
GSK3β 45 kDa
actin 43 kDa

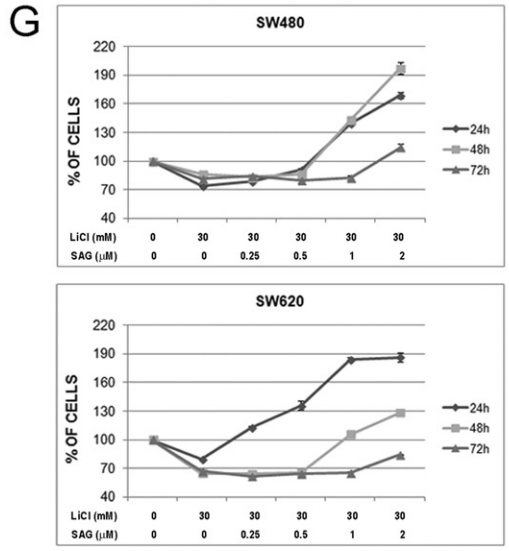
G
SW480
% OF CELLS
220
190
160
130
100
70
40
24h
48h
72h
LiCl (mM) 0 30 30 30 30 30
SAG (μM) 0 0 0.25 0.5 1 2
SW620
% OF CELLS
220
190
160
130
100
70
40
24h
48h
72h
LiCl (mM) 0 30 30 30 30 30
SAG (μM) 0 0 0.25 0.5 1 2

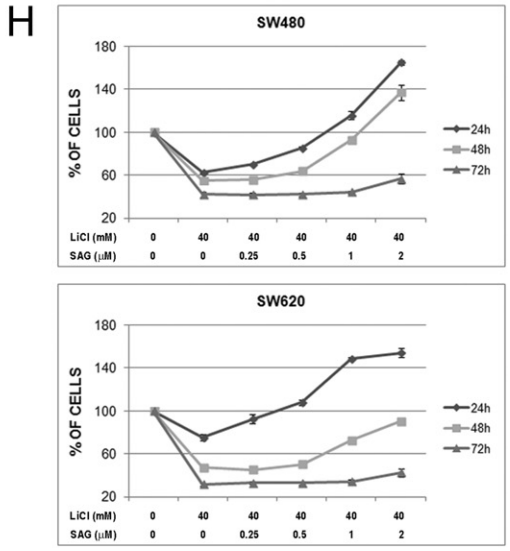
H
SW480
% OF CELLS
180
140
100
60
20
24h
48h
72h
LiCl (mM) 0 40 40 40 40 40
SAG (μM) 0 0 0.25 0.5 1 2
SW620
% OF CELLS
180
140
100
60
20
24h
48h
72h
LiCl (mM) 0 40 40 40 40 40
SAG (μM) 0 0 0.25 0.5 1 2

GSK3β Ser9 phosphorylation is indeed relevant for the LiCl-dependent decrease of Hh-Gli signaling and cellular proliferation, and that SAG can rescue the effects of LiCl by modifying the Ser9 phosphorylation of GSK3β. To check whether LiCl is able to restore the ability of GSK3β to phosphorylate Gli3, we tested the dynamics of the SuFu–Gli3–GSK3β complex formation after treatment, which is essential for proper Gli3 phosphorylation and cleavage. Immunofluorescent staining of GSK3β and Gli3 in SW480 and SW620 cells indicated changes in localization of these proteins in relation to each other after treatment with LiCl. In non-treated cells Gli3 was found both in the nucleus and cytoplasm, whereas GSK3β was located in the cytoplasm. Although there was a basal level of co-localization between these two proteins, an increase in co-localization was detected after treatment with 20 mM of LiCl for 16 h, implying that under these conditions GSK3β might phosphorylate Gli3 more efficiently than in non-treated conditions (Fig. 4C). Co-immunoprecipitation analyses in SW480 cells confirmed that indeed, SuFu binds Gli3, as well as GSK3β more efficiently after LiCl treatment. This complex already forms 10 h after treatment, whereas 24 h post-treatment Gli3 is already efficiently cleaved (Figs. 4D, 3E).

3.5. Inhibition of Hh-Gli signaling with LiCl induces autophagy and apoptosis

To determine the mechanism of cell death that occurs after inhibition with LiCl we tested the cells for autophagy and apoptosis. Acridine-orange staining revealed that this treatment significantly induced acidic vesicular organelle (AVO) formation in a dose-dependent manner (Fig. 5A, B), which is a characteristic of autophagy. To check whether autophagic flux is occurring, LC3 processing after LiCl treatment was analyzed, in the presence and absence of NH_4Cl, a lysosomal protease inhibitor. In SW480 cells 30 mM of LiCl did not increase LC3-II levels, but addition of NH_4Cl significantly increased LC3-II levels. No increase in LC3-II levels after LiCl treatment indicates that intra-autophagosomal LC3-II becomes rapidly degraded in autolysosomes, since after blocking lysosomal protease LC3-II levels increase (Fig. 5C) [31,32]. In SW620 cells however, an increase in LC3-II was visible after treatment with 30 mM of LiCl, and an additional increase in the presence of inhibitor. Therefore, these results indicate that autophagic flux is occurring under these conditions (Fig. 5D). Analysis of caspase-3 and PARP cleavage also indicate apoptosis induction with LiCl in SW480 cells (Fig. 5E). As for SW620 cells, only cleavage of PARP was detected at the dose of 40 mM of LiCl but not that of caspase-3 (Fig. 5F).

4. Discussion

Colon cancer is the third most commonly diagnosed cancer in males and the second in females [33]. Despite the efforts to optimize diagnostic processes and improve treatment regimens the mortality rate is still high [34]. These facts emphasize the need for improving our understanding of this disease and thereby provide new insights for future therapy design. To date several studies have addressed the activation of Hh-Gli signaling in colon cancer [9,35–37], some describe Gli1 and/or Gli2 as the main molecular switch in colon carcinogenesis [35,36,38], while others indicated a key role for Gli3 [37]. We showed expression of all Hh-Gli signaling components in a set of colon cancer clinical samples, with GSK3β and Gli3 showing high staining intensities (2 and 3) in 95% of samples. GSK3β expression positively correlated with DUKES' stage, whereas the same trend was visible for Gli3 although not statistically significant ($P = 0.058$). It should be noted that our set of clinical samples was consisted mostly of grade I tumors and only one sample of grade III colon cancer, with different DUKES' stages. Therefore, a larger set of samples with higher grade tumors should be assessed to confirm that these observations are not limited to this subpopulation of tumors.

Based on clinical data, we decided to investigate the role of GSK3β and Hh-Gli signaling more closely. In recent years it has become evident that GSK3β can have an altered, oncogenic role in certain tumor types [39–41]. This has also been confirmed for colon cancer [16,20], but the underlying mechanism of its function has not been elucidated. This study demonstrates a potential mechanism for deregulated GSK3β in colon cancer cells. We propose that it upregulates the Hh-Gli signaling pathway, which ensures cancer cell proliferation and survival. We found active Hh-Gli signaling in two colon cancer cell lines, which did not respond to classical inhibition with cyclopamine. The inability of cyclopamine to inhibit the Hh-Gli pathway in these cell lines is in agreement with observations in another study where the authors found components of the Hh-Gli signaling pathway in colon cancer cell lines, but could not inhibit it with cyclopamine [42]. As cyclopamine targets Smo it is evident that a deregulated GSK3β, which acts downstream of Smo, could block the effect of cyclopamine. On the other hand, LiCl, which targets GSK3β, downregulates Hh-Gli signaling. We show that this is a consequence of enhanced Gli3 processing into transcriptional repressor form (Gli3R). This, in turn, decreases cell proliferation and their clonogenic ability. Interestingly, this effect of LiCl on cell proliferation can be rescued by simultaneously stimulating the Hh-Gli signaling pathway, indicating a key role for this pathway in regulating proliferation of these two colon cancer cell lines. Since we showed that the Ser9-phosphorylated portion of GSK3β increases after LiCl treatment, we hypothesized, that this event restores the balance between the activating and inactivating phosphorylation on GSK3β, and enables it to properly phosphorylate Gli3. We confirmed that the Ser9 phosphorylation of GSK3β is indeed relevant for the LiCl-dependent decrease of Hh-Gli signaling activity and cell proliferation, since activation of the pathway with SAG is able to rescue the LiCl increase of Ser9 phosphorylation in both colon cancer cell lines. Immunofluorescent staining shows higher levels of Gli3 and GSK3β co-localization after treatment with LiCl which implies more efficient Gli3 phosphorylation, which is necessary for it to become cleaved [43]. This is supported with co-immunoprecipitation experiments which have shown that LiCl enhances Gli3–SuFu–GSK3β complex formation and thus Gli3 phosphorylation and processing (represented schematically in Fig. 6).

In contrast to inhibiting GSK3β with LiCl, knock-down of GSK3β led to Hh-Gli pathway activation, indicating that, in the aspect of treatment, it is crucial to restore GSK3β function in these cancer cells, rather than abolish its expression.

We also investigated how cell proliferation decreases after LiCl treatment. After Hh-Gli pathway inhibition with LiCl a significant increase in AVO formation is observed, which characterizes autophagy. Analysis of LC3 processing supported this finding, indicating induction of autophagic flux. It is known that lithium itself can activate autophagy through inhibition of inositol monophosphatase [44], but it remains to be investigated whether inhibition of Hh-Gli signaling, or more precisely Gli3R, may play a part as well. As Gli3 becomes processed after LiCl treatment it may no longer be able to inhibit autophagy, or may start repressing inhibitors of autophagy. Recent findings show that Hh-Gli signaling can regulate autophagy through Gli1 [45] or Gli2 [46]. Both groups found that inhibition of the pathway induced autophagy whereas activation of the pathway inhibited it. Even though autophagy is a conserved

Fig. 4. LiCl increases GSK3β Ser9 phosphorylation and enhances Gli3–GSK3β–SuFu complex formation. (A) Western blot of Ser9 phosphorylated GSK3β showing an increase after LiCl treatment compared with total GSK3β which remains constant. (B)Western blot of Ser9 phosphorylated GSK3β after treatment with 30 mM of LiCl, 0.5 μM of SAG, 1 μM of SAG and combinations of 30 mM of LiCl with 0.5 μM of SAG and 1 μM of SAG. SAG itself mildly decreases the Ser9 phosphorylated fraction of GSK3β compared with vehicle-treated cells, and is also able to rescue the LiCl induced increase in Ser9 phosphorylation. (C) Immunofluorescent analysis of Gli3 (red) and GSK3β (green) localization. Nuclei are stained with DAPI and shown in blue. In untreated cells GSK3β and Gli3 show a basal level of co-localization, mostly diffused. After LiCl treatment the co-localization rate increases and is localized in distinct perinuclear areas. Scale bars represent 5 μm. Quantification of co-localization is shown on graphs next to the images. (D) Western blot images of co-immunoprecipitation experiments, showing increased binding of Gli3 and Sufu, as well as GSK3β and SuFu after LiCl treatment. Optical density quantification of bands is shown on graphs below. NC — negative control.

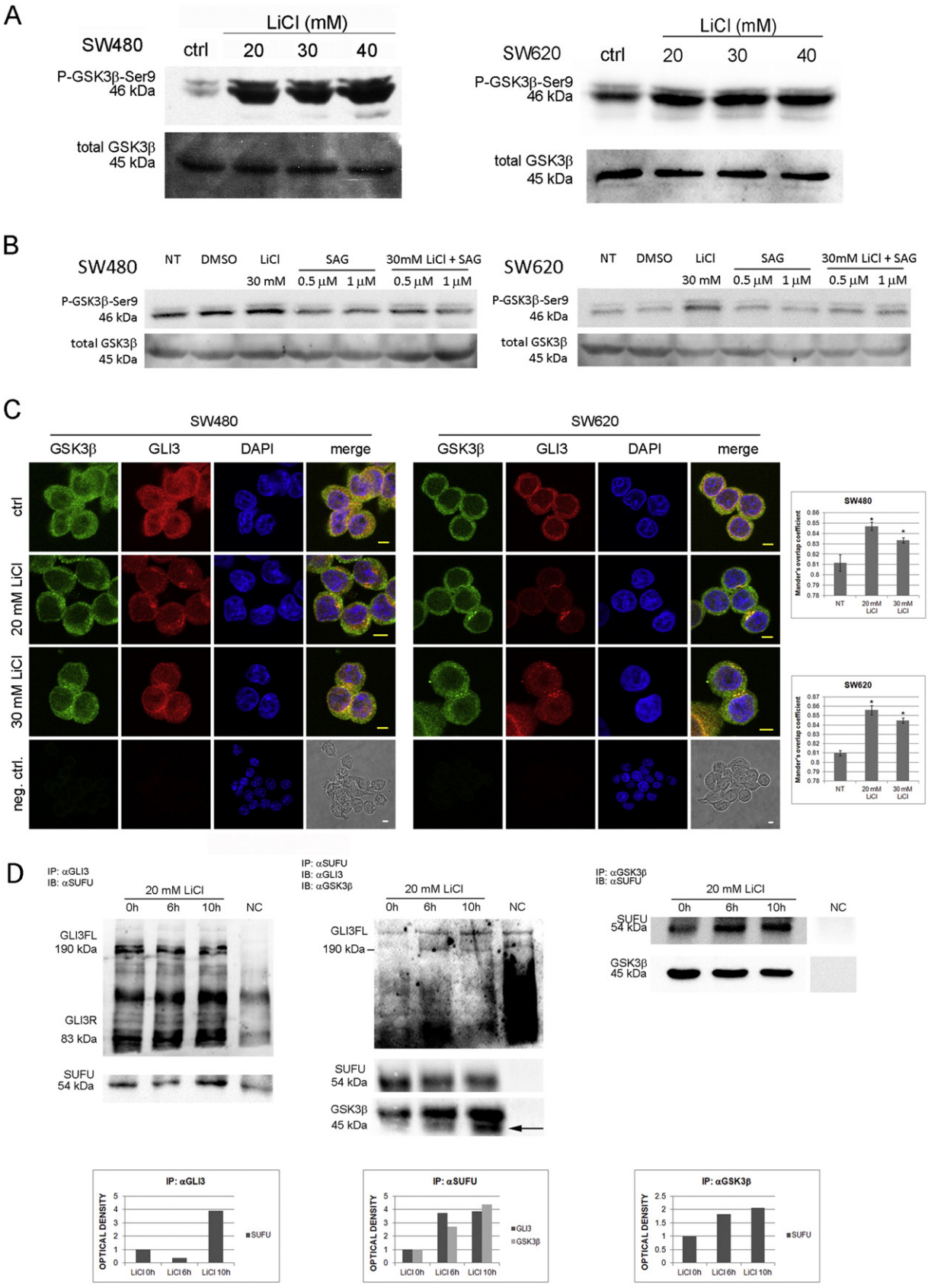
A
SW480
LiCl (mM)
ctrl 20 30 40
P-GSK3β-Ser9 46 kDa
total GSK3β 45 kDa
SW620
LiCl (mM)
ctrl 20 30 40
P-GSK3β-Ser9 46 kDa
total GSK3β 45 kDa
B
SW480
NT DMSO LiCl SAG 30mM LiCl + SAG
30 mM 0.5 μM 1 μM 0.5 μM 1 μM
P-GSK3β-Ser9 46 kDa
total GSK3β 45 kDa
SW620
NT DMSO LiCl SAG 30mM LiCl + SAG
30 mM 0.5 μM 1 μM 0.5 μM 1 μM
P-GSK3β-Ser9 46 kDa
total GSK3β 45 kDa
C
SW480
GSK3β GLI3 DAPI merge
SW620
GSK3β GLI3 DAPI merge
ctrl
20 mM LiCl
30 mM LiCl
neg. ctrl.
SW480
Mander's overlap coefficient
NT 20 mM LiCl 30 mM LiCl
SW620
Mander's overlap coefficient
NT 20 mM LiCl 30 mM LiCl
D
IP: αGLI3
IB: αSUFU
20 mM LiCl
0h 6h 10h NC
GLI3FL 190 kDa
GLI3R 83 kDa
SUFU 54 kDa
IP: αSUFU
IB: αGLI3
IB: αGSK3β
20 mM LiCl
0h 6h 10h NC
GLI3FL 190 kDa
SUFU 54 kDa
GSK3β 45 kDa
IP: αGSK3β
IB: αSUFU
20 mM LiCl
0h 6h 10h NC
SUFU 54 kDa
GSK3β 45 kDa
IP: αGLI3
OPTICAL DENSITY
LiCl 0h LiCl 6h LiCl 10h
SUFU
IP: αSUFU
OPTICAL DENSITY
LiCl 0h LiCl 6h LiCl 10h
GLI3
GSK3β
IP: αGSK3β
OPTICAL DENSITY
LiCl 0h LiCl 6h LiCl 10h
SUFU

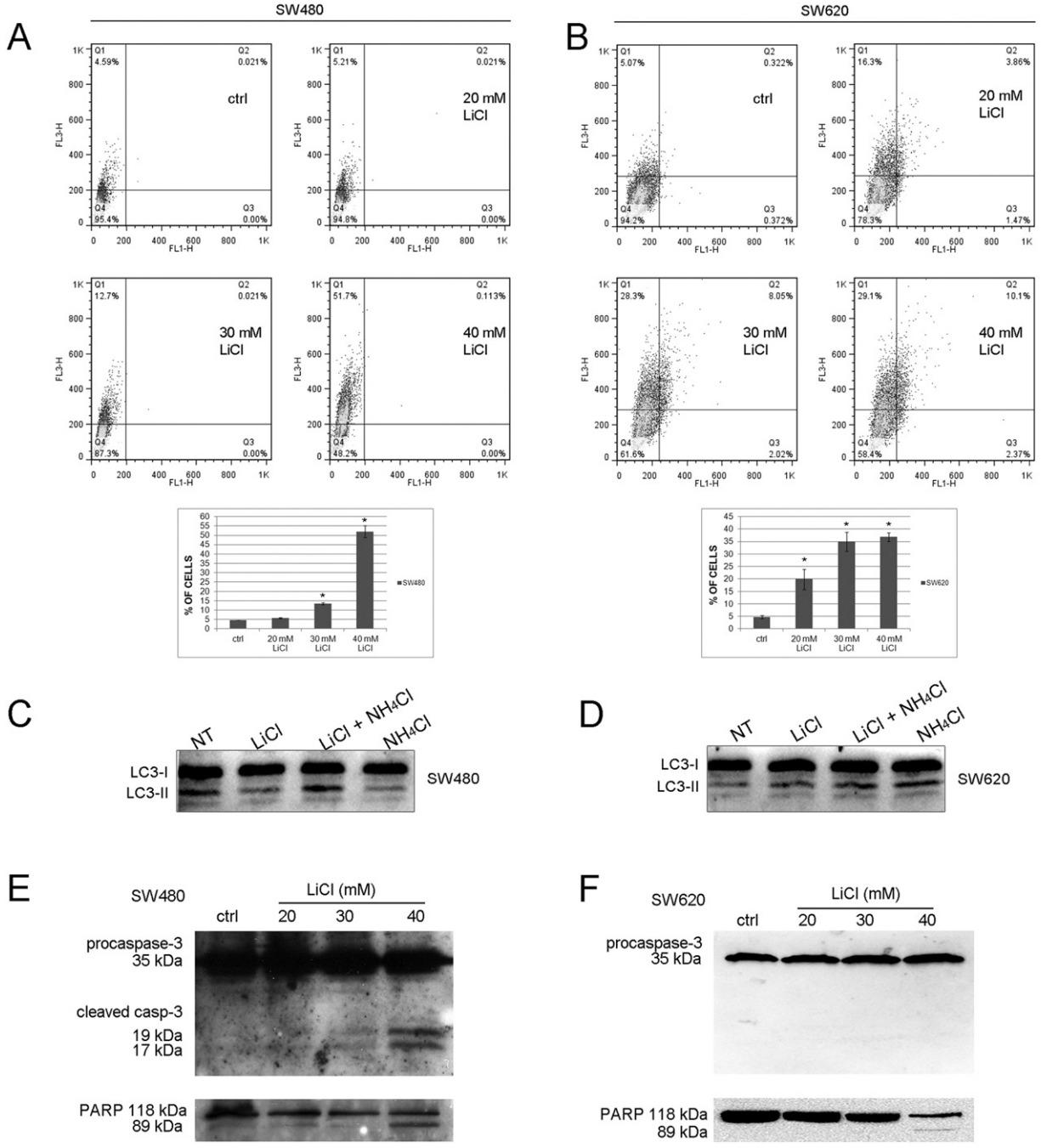

Fig. 5. LiCl induces autophagy and apoptosis in SW480 and SW620 cells. (A) Dot blot representations of flow cytometric analysis after acridine orange staining of SW480 cells, non-treated and treated with 20, 30 and 40 mM of LiCl with quantitative analysis shown on graph below. (B) Dot blot representations of flow cytometric analysis after acridine orange staining of SW620 cells, non-treated and treated with 20, 30 and 40 mM of LiCl with quantitative analysis shown on graph below. (C) Analysis of LC3 processing in SW480 cells after treatment with LiCl in the absence and in the presence of a lysosmal protease inhibitor. (D) Analysis of LC3 processing in SW620 cells after treatment with LiCl in the absence and in the presence of a lysosmal protease inhibitor. (E) Western blot analysis of caspase-3 and PARP cleavage indicating induction of apoptosis in SW480 cells after treatment with 30 and 40 mM of LiCl. (F) Western blot analysis of caspase-3 and PARP cleavage in SW620 cells showing only cleavage of PARP at 40 mM of LiCl.

process that enables cell survival under stressful conditions, it can also lead to cell death under certain conditions [47]. In our case autophagy results in cell death since a significant decrease in cell proliferation is observed. Also, induction of apoptosis was observed in SW480 cells, which suggests that autophagy may be providing the energy for the execution of apoptosis or cooperates with apoptosis to lead to cell death [48]. Gli3R has previously already been shown to increase levels of apoptosis in colon cancer cells [36]. As for SW620 cells, PARP cleavage was observed, but not that of caspase-3. It is possible that PARP is cleaved by another caspase that has not been tested [49] or independently of caspases [50].

This work implies that GSK3β is an interesting target for development of colon cancer therapeutics. Therapeutics directed toward the re-establishment of the inhibitory Ser9 phosphorylation are especially of interest since GSK3β knock-down activates Hh-Gli signaling, leading to potentially adverse effects. LiCl has been used for many years as therapy for mood disorders [51]. In fact, patients that have been treated with lithium for psychological reasons had lower risk of developing cancer compared with non-treated patients [52]. The problem with lithium is that it is used in supraphysiological concentrations in *in vitro* experiments and therefore the doses are not comparable to those used in patients. Recently, a group of authors reported that a novel GSK3β

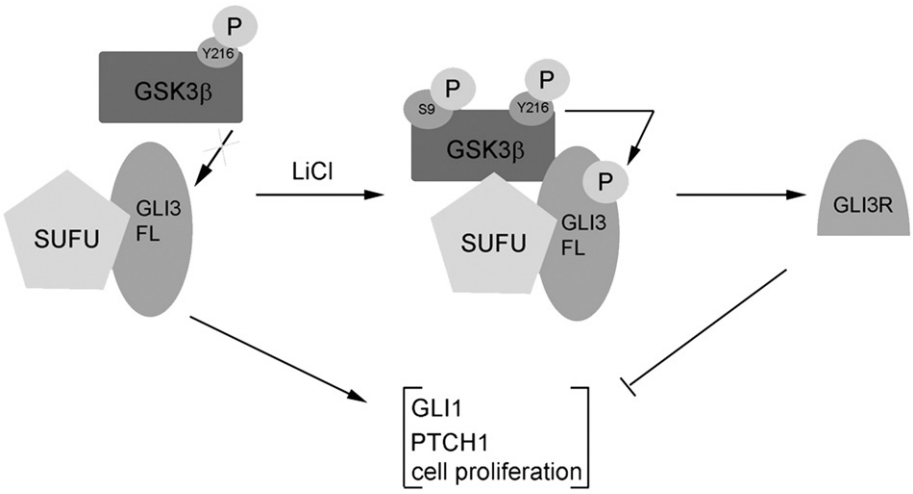

Fig. 6. Schematic representation of the proposed events in colon cancer cells before and after treatment with LiCl. GSK3β phosphorylated predominantly at Tyr216 is unable to phosphorylate Gli3 which thus stays in its full length activator form. LiCl promotes the Ser9 phosphorylation of GSK3β that restores the balance between the Tyr216 and Ser9 phosphorylation and enables GSK3β to function properly; it phosphorylates Gli3 and thereby promotes its processing into Gli3R, which downregulates the Hh-Gli pathway.

inhibitor, CG0009, induces cell death in breast cancer cells by enhancing the Ser9 phosphorylation, at concentrations much lower than those of LiCl [53]. On the other hand, blocking the Hh-Gli signaling pathway downstream of GSK3β may also represent an interesting approach of inhibiting cancer cell growth. This emphasizes the need for developing inhibitors specific for Gli3, which plays an important role in regulating the Hh-Gli pathway in our model.

Conflicts of interest

None.

Transparency document

The Transparency document associated with this article can be found, in the online version.

Acknowledgments

The authors wish to thank Dr. Sanja Kapitanović and Dr. Marijeta Kralj for the colon cancer cell lines, Dr. Marijeta Kralj and Dr. Ana-Matea Mikecin for help with autophagy analysis, Dr. Andreja Ambriović-Ristov for the α-PARP and α-caspase-3 antibodies, Lucija Horvat for help with confocal microscopy. We also wish to thank all the patients who participated in this study, Dr. Fabijan Knežević from the Sestre Milosrdnice University Hospital Center for the use of the autostainer and professor Romana Halapir Franković from the 5th High School (for math and science) in Zagreb for use of the microscope and camera. This study was funded by the Croatian Ministry of Science, Education and Sports (grant. no. 098-0982464-2461). The funding source had no role in the study design; in the collection, analysis and interpretation of data; in the writing of the report; and in the decision to submit the article for publication.

References

[1] P.W. Ingham, Hedgehog signaling in animal development: paradigms and principles, Genes Dev. 15 (2001) 3059–3087.
[2] M. Ramalho-Santos, D.A. Melton, A.P. McMahon, Hedgehog signals regulate multiple aspects of gastrointestinal development, Dev. Camb. Engl. 127 (2000) 2763–2772.
[3] H. Sasaki, Y. Nishizaki, C. Hui, M. Nakafuku, H. Kondoh, Regulation of Gli2 and Gli3 activities by an amino-terminal repression domain: implication of Gli2 and Gli3 as primary mediators of Shh signaling, Development 126 (1999) 3915–3924.
[4] B. Wang, J.F. Fallon, P.A. Beachy, Hedgehog-regulated processing of Gli3 produces an anterior/posterior repressor gradient in the developing vertebrate limb, Cell 100 (2000) 423–434.
[5] C.B. Bai, W. Auerbach, J.S. Lee, D. Stephen, A.L. Joyner, Gli2, but not Gli1, is required for initial Shh signaling and ectopic activation of the Shh pathway, Dev. Camb. Engl. 129 (2002) 4753–4761.
[6] Y. Pan, C.B. Bai, A.L. Joyner, B. Wang, Sonic hedgehog signaling regulates Gli2 transcriptional activity by suppressing its processing and degradation, Mol. Cell. Biol. 26 (2006) 3365–3377.
[7] M.M. Cohen, The hedgehog signaling network, Am. J. Med. Genet. A 123A (2003) 5–28.
[8] B. Stecca, A. Ruiz i Altaba, Context-dependent regulation of the GLI code in cancer by hedgehog and non-hedgehog signals, J. Mol. Cell Biol. 2 (2010) 84–95.
[9] T. Mazumdar, J. DeVecchio, T. Shi, J. Jones, A. Agyeman, J.A. Houghton, Hedgehog signaling drives cellular survival in human colon carcinoma cells, Cancer Res. 71 (2011) 1092–1102.
[10] P. Kogerman, T. Grimm, L. Kogerman, D. Krause, A.B. Undén, B. Sandstedt, R. Toftgård, P.G. Zaphiropoulos, Mammalian suppressor-of-fused modulates nuclear-cytoplasmic shuttling of Gli-1, Nat. Cell Biol. 1 (1999) 312–319.
[11] Y. Kise, A. Morinaka, S. Teglund, H. Miki, Sufu recruits GSK3beta for efficient processing of Gli3, Biochem. Biophys. Res. Commun. 387 (2009) 569–574.
[12] M. Merchant, F.F. Vajdos, M. Ultsch, H.R. Maun, U. Wendt, J. Cannon, W. Desmarais, R.A. Lazarus, A.M. De Vos, F.J. De Sauvage, Suppressor of fused regulates Gli activity through a dual binding mechanism, Mol. Cell. Biol. 24 (2004) 8627–8641.
[13] L. Kim, A.R. Kimmel, GSK3 at the edge: regulation of developmental specification and cell polarization, Curr. Drug Targets 7 (2006) 1411–1419.
[14] K. Takenaka, Y. Kise, H. Miki, GSK3 [beta] positively regulates Hedgehog signaling through Sufu in mammalian cells, Biochem. Biophys. Res. Commun. 353 (2007) 501–508.
[15] L. Meijer, M. Flajolet, P. Greengard, Pharmacological inhibitors of glycogen synthase kinase 3, Trends Pharmacol. Sci. 25 (2004) 471–480.
[16] A. Shakoori, W. Mai, K. Miyashita, K. Yasumoto, Y. Takahashi, A. Ooi, K. Kawakami, T. Minamoto, Inhibition of GSK-3 beta activity attenuates proliferation of human colon cancer cells in rodents, Cancer Sci. 98 (2007) 1388–1393.
[17] B.W. Doble, J.R. Woodgett, GSK-3: tricks of the trade for a multi-tasking kinase, J. Cell Sci. 116 (2003) 1175–1186.
[18] R.S. Jope, G.V. Johnson, The glamour and gloom of glycogen synthase kinase-3, Trends Biochem. Sci. 29 (2004) 95–102.
[19] J. Luo, Glycogen synthase kinase 3β (GSK3β) in tumorigenesis and cancer chemotherapy, Cancer Lett. 273 (2009) 194–200.
[20] A. Shakoori, A. Ougolkov, Z.W. Yu, B. Zhang, M.H. Modarressi, D.D. Billadeau, M. Mai, Y. Takahashi, T. Minamoto, Deregulated GSK3β activity in colorectal cancer: its association with tumor cell survival and proliferation, Biochem. Biophys. Res. Commun. 334 (2005) 1365–1373.
[21] N.-A. Pham, A. Morrison, J. Schwock, S. Aviel-Ronen, V. Iakovlev, M.-S. Tsao, J. Ho, D.W. Hedley, Quantitative image analysis of immunohistochemical stains using a CMYK color model, Diagn. Pathol. 2 (2007) 8.
[22] C.M. Bailey, D.E. Abbott, N.V. Margaryan, Z. Khalkhali-Ellis, M.J.C. Hendrix, Interferon regulatory factor 6 promotes cell cycle arrest and is regulated by the proteasome in a cell cycle-dependent manner, Mol. Cell. Biol. 28 (2008) 2235–2243.
[23] C.M. Bailey, N.V. Margaryan, D.E. Abbott, B.C. Schutte, B. Yang, Z. Khalkhali-Ellis, M.J.C. Hendrix, Temporal and spatial expression patterns for the tumor suppressor maspin and its binding partner interferon regulatory factor 6 during breast development, Develop. Growth Differ. 51 (2009) 473–481.
[24] D. Leovic, M. Sabol, P. Ozretic, V. Musani, D. Car, K. Marjanovic, V. Zubcic, I. Sabol, M. Sikora, M. Grce, L. Glavas-Obrovac, S. Levanat, Hh-Gli signaling pathway activity in oral and oropharyngeal squamous cell carcinoma, Head Neck 34 (2012) 104–112.
[25] A. Koch, A. Waha, W. Hartmann, U. Milde, C.G. Goodyer, N. Sörensen, F. Berthold, B. Digon-Söntgerath, J. Krätzschmar, O.D. Wiestler, T. Pietsch, No

evidence for mutations or altered expression of the Suppressor of Fused gene (SUFU) in primitive neuroectodermal tumours, Neuropathol. Appl. Neurobiol. 30 (2004) 532–539.
[26] M. Tojo, H. Kiyosawa, K. Iwatsuki, K. Nakamura, F. Kaneko, Expression of the GLI2 oncogene and its isoforms in human basal cell carcinoma, Br. J. Dermatol. 148 (2003) 892–897.
[27] R. Sacedón, A. Varas, C. Hernández-López, C. Gutiérrez-deFrías, T. Crompton, A.G. Zapata, A. Vicente, Expression of Hedgehog proteins in the human thymus, J. Histochem. Cytochem. 51 (2003) 1557–1566.
[28] G.N. Pandey, Y. Dwivedi, H.S. Rizavi, T. Teppen, G.L. Gaszner, R.C. Roberts, R.R. Conley, GSK-3beta gene expression in human postmortem brain: regional distribution, effects of age and suicide, Neurochem. Res. 34 (2009) 274–285.
[29] M. Sabol, D. Car, V. Musani, P. Ozretic, S. Oreskovic, I. Weber, S. Levanat, The Hedgehog signaling pathway in ovarian teratoma is stimulated by Sonic Hedgehog which induces internalization of Patched, Int. J. Oncol. 41 (2012) 1411–1418.
[30] R.S. Jope, Lithium and GSK-3: one inhibitor, two inhibitory actions, multiple outcomes, Trends Pharmacol. Sci. 24 (2003) 441–443.
[31] I. Tanida, N. Minematsu-Ikeguchi, T. Ueno, E. Kominami, Lysosomal turnover, but not a cellular level, of endogenous LC3 is a marker of autophagy, Autophagy 1 (2005) 84–91.
[32] K. Sato, K. Tsuchihara, S. Fujii, M. Sugiyama, T. Goya, Y. Atomi, T. Ueno, A. Ochiai, H. Esumi, Autophagy is activated in colorectal cancer cells and contributes to the tolerance to nutrient deprivation, Cancer Res. 67 (2007) 9677–9684.
[33] A. Jemal, F. Bray, M.M. Center, J. Ferlay, E. Ward, D. Forman, Global cancer statistics, CA Cancer J. Clin. 61 (2011) 69–90.
[34] M.S. Reimers, E.C.M. Zeestraten, P.J.K. Kuppen, G.J. Liefers, C.J.H. van de Velde, Biomarkers in precision therapy in colorectal cancer, Gastroenterol. Rep. 1 (2013) 166–183.
[35] T. Mazumdar, J. Devecchio, A. Agyeman, T. Shi, J.A. Houghton, The GLI genes as the molecular switch in disrupting Hedgehog signaling in colon cancer, Oncotarget 2 (2011) 638–645.
[36] F. Varnat, A. Duquet, M. Malerba, M. Zbinden, C. Mas, P. Gervaz, A. Ruiz i Altaba, Human colon cancer epithelial cells harbour active HEDGEHOG-GLI signalling that is essential for tumour growth, recurrence, metastasis and stem cell survival and expansion, EMBO Mol. Med. 1 (2009) 338–351.
[37] H.N. Kang, S.C. Oh, J.S. Kim, Y.A. Yoo, Abrogation of Gli3 expression suppresses the growth of colon cancer cells via activation of p53, Exp. Cell Res. 318 (2011) 539–549.
[38] M. Xu, X. Li, T. Liu, A. Leng, G. Zhang, Prognostic value of hedgehog signaling pathway in patients with colon cancer, Med. Oncol. 2 (2012) 1010–1016.
[39] Q. Cao, X. Lu, Y.-J. Feng, Glycogen synthase kinase-3β positively regulates the proliferation of human ovarian cancer cells, Cell Res. 16 (2006) 671–677.
[40] M. Kunnimalaiyaan, A.M. Vaccaro, M.A. Ndiaye, H. Chen, Inactivation of glycogen synthase kinase-3beta, a downstream target of the raf-1 pathway, is associated with growth suppression in medullary thyroid cancer cells, Mol. Cancer Ther. 6 (2007) 1151–1158.
[41] M.O. Nowicki, N. Dmitrieva, A.M. Stein, J.L. Cutter, J. Godlewski, Y. Saeki, M. Nita, M.E. Berens, L.M. Sander, H.B. Newton, Lithium inhibits invasion of glioma cells; possible involvement of glycogen synthase kinase-3, Neuro-Oncology 10 (2008) 690–699.
[42] G. Chatel, C. Ganeff, N. Boussif, L. Delacroix, A. Briquet, G. Nolens, R. Winkler, Hedgehog signaling pathway is inactive in colorectal cancer cell lines, Int. J. Cancer 121 (2007) 2622–2627.
[43] D. Tempe, M. Casas, S. Karaz, M.-F. Blanchet-Tournier, J.-P. Concordet, Multisite Protein kinase a and Glycogen synthase kinase 3 beta phosphorylation leads to Gli3 ubiquitination by SCF bTrCP, Mol. Cell. Biol. 26 (2006) 4316–4326.
[44] S. Sarkar, Lithium induces autophagy by inhibiting inositol monophosphatase, J. Cell Biol. 170 (2005) 1101–1111.
[45] Y. Wang, C. Han, L. Lu, S. Magliato, T. Wu, Hedgehog signaling pathway regulates autophagy in human hepatocellular carcinoma cells: hepatology, Hepatology 58 (2013) 995–1010.
[46] M. Jimenez-Sanchez, F.M. Menzies, Y.-Y. Chang, N. Simecek, T.P. Neufeld, D.C. Rubinsztein, The Hedgehog signalling pathway regulates autophagy, Nat. Commun. 3 (2012) 1200.
[47] A. Eisenberg-Lerner, A. Kimchi, The paradox of autophagy and its implication in cancer etiology and therapy, Apoptosis 14 (2009) 376–391.
[48] A. Eisenberg-Lerner, S. Bialik, H.U. Simon, A. Kimchi, Life and death partners: apoptosis, autophagy and the cross-talk between them, Cell Death Differ. 16 (2009) 966–975.
[49] M. Germain, E.B. Affar, D. D'Amours, V.M. Dixit, G.S. Salvesen, G.G. Poirier, Cleavage of automodified poly (ADP-ribose) polymerase during apoptosis evidence for involvement of caspase-7, J. Biol. Chem. 274 (1999) 28379–28384.
[50] P. Masdehors, Ubiquitin-dependent protein processing controls radiation-induced apoptosis through the N-end rule pathway, Exp. Cell Res. 257 (2000) 48–57.
[51] R.S. Jope, C.J. Yuskaitis, E. Beurel, Glycogen synthase kinase-3 (GSK3): inflammation, diseases, and therapeutics, Neurochem. Res. 32 (2007) 577–595.
[52] Y. Cohen, A. Chetrit, P. Sirota, B. Modan, Cancer morbidity in psychiatric patients: influence of lithium carbonate treatment, Med. Oncol. 15 (1998) 32–36.
[53] H.M. Kim, C.-S. Kim, J.-H. Lee, S.J. Jang, J.J. Hwang, S. Ro, J. Choi, CG0009, a novel Glycogen synthase kinase 3 inhibitor, induces cell death through cyclin D1 depletion in breast cancer cells, PLoS ONE 8 (2013), e60383.